Active Feedback Stabilization of the Resistive Wall Mode on the DIII D-Device

M. Okabayashi, J. Bialek, M. S. Chance, M. S. Chu, E. D. Fredrickson, A. M. Garofalo, M. Gryaznevich, R. E. Hatcher, T. H. Jensen, L. C. Johnson, R. J. Lahaye, E. A. Lazarus, M. A. Makowski, J. Manickam, G. A. Navratil, J. T. Scoville, E. J. Strait, A. D. Turnbull, M. L. Walker,

U.S. Department of Energy

Lawrence
Livermore
National
Laboratory

November 1, 2000

ACTIVE FEEDBACK STABILIZATION OF THE RESISTIVE WALL MODE ON THE DIII–D DEVICE

by
M. OKABAYASHI, J. BIALEK, M.S. CHANCE, M.S. CHU, E.D. FREDRICKSON,
A.M. GAROFALO, M. GRYAZNEVICH, R.E. HATCHER, T.H. JENSEN,
L.C. JOHNSON, R.J. LAHAYE, E.A. LAZARUS, M.A. MAKOWSKI,
J. MANICKAM, G.A. NAVRATIL, J.T. SCOVILLE, E.J. STRAIT, A.D. TURNBULL,
M.L. WALKER, and The DIII–D TEAM

NOVEMBER 2000

DISCLAIMER

ACTIVE FEEDBACK STABILIZATION OF THE RESISTIVE WALL MODE ON THE DIII–D DEVICE

by

M. OKABAYASHI,* J. BIALEK,† M.S. CHANCE,* M.S. CHU, E.D. FREDRICKSON,*
A.M. GAROFALO,† M. GRYAZNEVICH,‡ R.E. HATCHER,* T.H. JENSEN,
L.C. JOHNSON,* R.J. LAHAYE, E.A. LAZARUS,# M.A. MAKOWSKI,△
J. MANICKAM,* G.A. NAVRATIL,† J.T. SCOVILLE, E.J. STRAIT, A.D. TURNBULL,
M.L. WALKER, and The DIII–D TEAM

*Princeton Plasma Physics Laboratory, Princeton, New Jersey.
†Columbia University, New York, New York.
‡UKAEA-Culham Laboratory, Abingdon, United Kingdom.
#Oak Ridge National Laboratory, Oak Ridge, Tennessee.
△Lawrence Livermore National Laboratory, Livermore, California.

ABSTRACT

A proof of principle magnetic feedback stabilization experiment has been carried out to suppress the resistive wall mode (RWM), a branch of the ideal magnetohydrodynamic (MHD) kink mode under the influence of a stabilizing resistive wall, on the DIII-D tokamak device [Plasma Phys. and Contr. Fusion Research (International Atomic Energy Agency, Vienna, 1986), p. 159]. The RWM was successfully suppressed and the high beta duration above the no wall limit was extended to more than 50 times the resistive wall flux diffusion time. It was observed that the mode structure was well preserved during the time of the feedback application. Several lumped parameter formulations were used to study the feedback process. The observed feedback characteristics are in good qualitative agreement with the analysis. These results provide encouragement to future efforts towards optimizing the RWM feedback methodology in parallel to what has been successfully developed for the $n = 0$ vertical positional control. Newly developed MHD codes have been extremely useful in guiding the experiments and in providing possible paths for the next step.

I. INTRODUCTION

From the beginning of fusion research, ideal magnetohydrodynamic (MHD) instabilities have been considered to be one of the most dangerous instabilities preventing achievement of high-performance plasma configurations. Within the last decade, various experiments have consistently indicated that the ideal MHD kink instability plays a significant role in the operational limits of Reversed Field Pinches (RFP), Spheromaks, Field Reversed Configurations (FRC), and Tokamaks.[1–3] With the achievement of the high-pressure collisionless regime in tokamaks, and with the significant improvement in MHD diagnostics, understanding of the ideal kink instability has greatly advanced and matured. Stabilization of the plasma to the ideal MHD instabilities predicted from the linear ideal MHD theory has become one of the prerequisites of fusion devices.

Ideal MHD theory predicts that a nearby perfectly conducting wall would allow tokamak operation with extremely high beta plasmas: for example, for the DIII-D tokamak, the theory predicts normalized beta values, $\beta_N = \beta/(I/aB) \approx 5\text{–}6$ (%-T-m/MA). These high β_N values are fundamental to the advanced tokamak concept.[4] However, due to the finite resistivity of the first wall, these high β_N values can only be sustained for a short period of time before a sub-branch the resistive wall mode (RWM) is excited. The characteristics of this RWM are such that it has a real frequency and growth rate comparable to τ_w^{-1}. Here, τ_w is the resistive flux penetration time of the wall,[5] typically about 5 ms in DIII-D. Experimentally, the RWM has been observed in several tokamaks: DIII–D,[6] Princeton Beta Experiment Modified (PBXM),[7] and High Beta Tokamak-Extended Pulse (HBT-EP).[8] Therefore, stabilization of a high β tokamak plasma against the RWM is one of the most urgent topics in fusion research.

In the DIII–D device, the RWM was first discovered in discharges during the exploration of high β regimes.[6,9] In the pre-RWM phase of these discharges, a high β condition was first sustained transiently. The β value in this phase was approximately 30% higher than the predicted beta limit given by ideal MHD stability calculations with the assumption of no conducting wall. A detailed examination of the dynamic evolution of the plasma revealed that when β_N approaches $\beta_{N.no\text{-wall}}$, the amplitude of the RWM increases slowly, (with growth rate $\gamma \ll 1/\tau_w$) in conjunction with a slow decrease of the toroidal plasma rotation, leading to β collapse.[9,10] The slowing down of the plasma has been conjectured as the event leading to the growth of the RWM. This observation led to a series of experimental studies of the angular momentum inputs to the plasma. These include the torque exerted by the saturated RWM, momentum input from the neutral beam, and the drag due to small uncompensated error fields.[11–13] The observations of the initial small RWM growth with low amplitudes followed by the sudden transition to a fast

growth phase was qualitatively consistent with a hypothesis of the torque balance scenario proposed by Gimblett and Hastie.[14] Since even a small amplitude RWM could cause the plasma to slow down and this in turn allows the RWM to grow to large amplitude and leads to β collapse, a mechanism to stabilize the RWM without relying solely on plasma rotation is needed.

We report here on a proof-of-principle experiment that was conducted for the stabilization of RWM using magnetic field feedback control. Our objective is the demonstration of the technical ability to control the RWM with an active magnetic feedback system which makes the resistive wall and sensor combination act like a perfect conducting wall. The key to the possibility of this method of stabilization is the recognition that the growth rate and rotation frequency of the resistive wall mode have been lowered by the resistive wall to the inverse of the resistive flux diffusion time scale

Experimentally, the parametric dependence of feedback stabilization has been examined using discharges with a rapid plasma current ramp. Utilizing feedback, the duration of the high β_N period was increased to at least 50 times τ_w. Experimental results also indicate that during feedback the internal and external poloidal mode structures are well preserved, supporting the rigid displacement assumption used in the various RWM simulation models. In this work, we summarize several proposed lumped parameter formulations[15–18] for the RWM. Partial motivation for this approach is prior success with lumped parameter model in design of the $n = 0$ vertical positional control.[19] Predictions from these models were used to compare the major parametric dependencies of the feedback logic with the experimental results. We found that these lumped parameter formulations, despite their lack of detail, were able to qualitatively explain the major parametric variations in the experimental observations. On the other hand, we also present more rigorous aspects of the simulation: theoretical prediction of the mode structure and mode rigidity derived from a newly developed VACUUM+GATO code.[20,21] Furthermore, more detailed issues of RWM feedback stabilization and future plans are presented via VALEN code predictions.[22]

II. BACKGROUND OF
RWM FEEDBACK STABILIZATION

In the 1990s research on high β tokamak plasmas was centered on the achievable β value in a steady-state reactor grade plasma. The relevant β value is one for which the plasma is not only ideal MHD stable with an ideal external wall but also stable when the resistivity of the external wall is taken into account — stable to the RWM. Major advances in this area were first obtained by Bondeson and Ward.[23,24] They discovered the possible existence of a completely stabilized tokamak operation regime for the RWM. The salient feature of this operation regime is characterized by the necessity of plasma rotation. According to their analysis, the resistive wall should be located in a stable zone just inside the limiting radius for the ideal kink but not too close to the plasma surface to avoid strong interaction with the plasma. Increasing the plasma toroidal rotation as shown in Fig. 1 can broaden the stable zone. The stabilization mechanism is momentum imparted to the RWM through the perturbed plasma viscosity. Increasing the plasma rotation will eventually impart enough momentum to the RWM to dislodge it from the resistive wall. The required rotation velocity for stabilization is moderate, a few percent of the Alfvén velocity on integer q (in particular, q = 2, 3) surfaces where the mode amplitude is expected to be large. The corresponding critical rotation frequency for present devices is up to the range of a few tens of kilohertz, which is achievable with the neutral beam power typically available. However, extrapolating from these analyses, the required rotation may be too high for reactor devices and to adopt rotation as the main RWM stabilizing mechanism requires the introduction of new techniques for angular momentum input. Nonetheless, this discovery has revitalized the effort for stabilization of global low-n kink modes and also pointed out an important issue of RWM physics. That is the
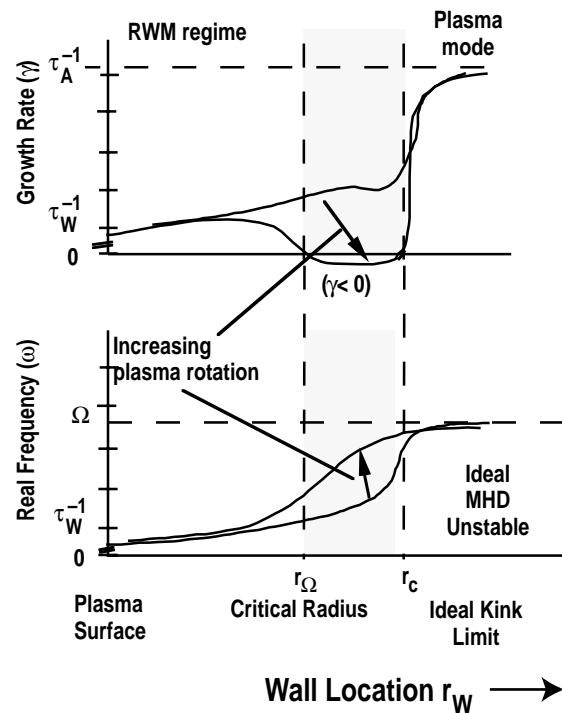
Fig. 1. The characteristics of resistive wall mode proposed by Bondeson and Ward:[23,24] growth rate and real frequency vs. wall location. The external kink mode is converted into a RWM when the wall is located within the ideal MHD limit radius, r_c. Ω is the plasma rotation and r_Ω is the critical radius for the stable zone.

maintenance of plasma rotation through the balance of the momentum input by the neutral beam, the torque exerted by the RWM mode and the natural loss of angular momentum through transport. Gimblett and Hastie subsequently provided insight into the non-linear process of RWM evolution with a self-consistent torque balance model.[14]

In DIII-D, the predicted existence of this stable regime for the RWM in neutral beam injection (NBI) heated discharges has been investigated. The NBI angular momentum input is varied by varying the beam energy while holding the total NBI input power constant — hence maintaining the plasma pressure. (The plasma rotation was increased up to 30%–40% near q = 2.) In spite of the faster plasma rotation in the early phase of the discharge, later a delayed onset of the RWM invariably took place and the mode grows coincident with the gradual decrease of the plasma rotation velocity. Although the discharge duration was somewhat prolonged in comparison to the lower rotation case, RWM growth occurred when the plasma rotation decreased below the same critical value. The delay of the RWM onset with higher momentum input is certainly a promising observation. However, further delay of the RWM onset requires the increase of angular momentum input, which in turn will require more NBI power. This indicates that relying on higher plasma rotation alone without providing a means for maintaining this rotation may not be a viable path for RWM stabilization. Instead, rotation should be complemented with other stabilization schemes, such as magnetic feedback.

In should be pointed out that the feasibility of an alternative path for RWM stabilization was hidden in Bondeson's original study. Even if the stability window were not entered, a large parameter space exists in which the structure of the RWM is found to slip through the plasma and rotate with respect to the resistive wall with a time constant τ_w. The mode growth time is also in the τ_w range. This RWM, at this extremely low characteristic frequency, makes the approach of magnetic feedback a practical possibility. Bishop, Fitzpatrick and Jensen[25–27] have examined magnetic feedback approaches and suggested that magnetic feedback stabilization can be sufficiently effective and economically attractive even in reactor configurations. Since the RWM feedback stabilization coils are located relatively close to the vacuum wall, within 20%–30% of the plasma minor radius away from the wall, the power required to compensate for the flux loss is rather modest. Furthermore, these coils and power supplies can be utilized for other functions like error field correction and vertical positional control. In fact, on DIII-D the same set of coils and power supply are utilized for both RWM control and field error correction.

An analogy can be drawn between the feedback stabilization of the n = 1 RWM and the n = 0 vertical position instability. We note that in order to control the n = 0 vertical position in non-circular current carrying toroidal devices, a repertoire of experimental methodology has been successfully developed with many years of experience. Both the n = 0 vertical position control and n = 1 RWM feedback systems try to use active feedback coils to compensate for the resistive

flux loss caused by the deviation of the plasma equilibrium from the desired configuration. The difference is: the vertical positional feedback system replenishes the lost axisymmetric flux and the RWM feedback system replenishes the lost helical flux. Development of the vertical positional instability results in a sequence of axisymmetric vertically displaced equilibria. Development of the RWM results in a series of instantaneous helical equilibria with an additional helical field. The key to this analogy is that the time scale of the RWM instability evolution is similar to the resistive flux loss time, which is much longer than the Alfvénic MHD time scale.

However, one major difference is that for the n = 0 instability, the energy source for the instability always exists. It originates from the magnetic field curvature determined from the external vertical and shaping fields, fixed in time and space and in the lowest order does not depend sensitively on the plasma parameters. On the other hand, the principal energy source of the RWM instability originates from the plasma current and pressure profile. It is internally driven so that it is less easy to have an exact knowledge of the instability onset. Furthermore, being helical, the pattern of the RWM can be rotated to take up different phase angles in the toroidal direction. This adds another parameter to determine the state of the plasma and is an extra complication. Nonetheless, we found that feedback control of the RWM can be discussed in a frame work similar to what we use for the control of the n = 0 mode, provided that the mode structure can be assumed preserved during feedback and only its amplitude evolves in time. Specifically, an effective self-inductance can be introduced to represent the mode excitation energy source that gives rise to the "virtual" helical skin current. The helical skin current serves as an interface between the inside bulk plasma mode structure and the outside magnetic parameters which are readily measured. We found that the discussion of the feedback stabilization of the RWM is greatly facilitated through this analogy with the formulation used in the control of the n = 0 mode and through the accumulated intuition developed for control of the n = 0 mode.

III. THE LUMPED PARAMETER
FEEDBACK CIRCUIT EQUATIONS

There have been several formulations of the resistive wall mode dynamics and its applications utilizing the lumped parameter approach.[15-18] For instance, this approach has been used to optimize the feedback logic and to optimize the arrangement of sensors suitable for feedback stabilization of the RWM. The basic parametric dependencies can all be included and displayed in an effective manner within this model. Except for the definition of the plasma response, references 15 and 16 are identical in the cylindrical model limit. Both use the helical skin current response on the plasma surface (Skin Current Model). The concept of Ref. 15 has been further extended to a full, two-dimensional MHD model coupling with the VALEN code.[22] Liu and Bondeson[28] use Pade approximation to cast stability results from the MARS code into the lumped parameter model, making it possible to study the continuous variation of the stability characteristics of the feedback circuit. For experimental analysis in the present work, the formulations from the Jensen/Garofalo[18] model and the Skin Current model[16] are used.

First, the formulation of Ref. 16 is used to identify the major issues of the RWM feedback system. A lumped parameter model with a thin resistive wall approximation is given by:

$$L_{eff}I_p + M_{pw}I_w + M_{pc}I_c = 0 \quad , \tag{1}$$

$$M_{wp}\, dI_p/dt + L_w\, dI_w/dt + M_{wc}\, dI_c/dt + R_w\, I_w = 0 \quad , \tag{2}$$

$$\Psi_o = M_{op}\, I_p + M_{ow}\, I_w + M_{oc}\, I_c \quad , \tag{3}$$

$$Y = f(\Psi_o) \quad , \tag{4}$$

$$I_c = -(G/M_{oc})\, Y \text{ (for negative feedback, } G > 0) \quad , \tag{5}$$

where suffixes, p, w, c, o correspond to plasma, passive wall, active coil and observation sensor respectively. The M_{ij} are mutual inductances between these elements. I_p, I_w and I_c correspond to the plasma skin current, the passive wall eddy current, and the active coil current. L_{eff}, the effective self-inductance, characterizes the plasma response to the currents of I_w and I_c. L_{eff} includes, in particular, the internal ideal MHD plasma response and is less than the simple geometrical inductance due to the plasma response. Ψ_o represents the helical flux observed at the sensor location, Y is the input to the feedback controller and G is the total gain through the controller and power supply.

Standard sensors discussed in most of the references[15–18,25–28] have been designed to measure the total flux, which includes the flux from the plasma, the wall and the active coil currents [Eq. (3)]. There have been several proposed feedback logic schemes such as the Smart Shell,[25] the Fake Rotating Shell,[26,27] and the explicit mode logic. For clarity, here we define the feedback logic schemes used in the present experiments.

The Smart Shell logic uses the total flux Ψ_o as the controller input Y,

$$Y = \Psi_o \quad . \tag{6}$$

Since the observed flux Ψ_o [Eq. (3)] includes the flux at the sensor location which originates from the direct coupling to the active coil currents; and these currents could be unrelated to the RWM plasma response, it has been suggested that the total flux Ψ_o may not be the best choice as the feedback signal input. One alternate proposal is thus to use Ψ_o but with compensation for the flux due to the direct coupling. This is called the simple explicit mode logic.

$$Y = \Psi_o - M_{oc} I_c \quad . \tag{7}$$

It is also possible instead to compensate also for the flux due to eddy currents on the resistive wall induced by the coil currents, or with

$$Y = \Psi_o - M_{oc} I_c F \tag{8}$$

In Eq. (8), the quantity F is given, for simplicity, in Laplace transform notation by,

$$F = 1 - (M_{ow} M_{wc}/M_{oc} L_w) [s \tau_w/(1 + s \tau_w)] \quad . \tag{9}$$

We note that in notation adopted in Laplace transforms, $s = i\omega + \gamma$. Thus in Eq. (8), the input to the controller Y is flux associated only with the plasma mode. This scheme is called full explicit mode logic.

For these Smart Shell and explicit mode logic schemes, the feedback stability is expressed in Laplace transform notation as

$$-s \gamma_o^{-1} + 1 = -G(\Delta + \hat{M}_{oc}/M_{oc})/[1 - G (F + \Delta)] \quad . \tag{10}$$

where $\hat{M}_{wp} = M_{wp} - M_{wo}M_{op}/L_{eff}$, $\hat{M}_{ow} = M_{ow} - M_{op}M_{pw}/L_{eff}$, $\hat{L}_w = L_w - M_{wp}M_{pw}/L_{eff}$, and $\hat{M}_{oc} = M_{oc} - M_{op} M_{pc}/L_{eff}$. For a plasma-wall condition unstable to the RWM, $\hat{M}_{ow}, \hat{M}_{wp}, \hat{M}_{oc}$ are negative.[16] In Eq. (10), the open loop growth rate γ_o is given by

$$\gamma_o^{-1} = -\tau_w (1 - M_{wp} M_{pw}/L_w L_{eff}) \quad . \tag{11}$$

Here, γ_o^{-1} represents the growth time of the RWM, with no feedback applied, and

$$\Delta = -(\hat{L}_w \, \hat{M}_{oc} - \hat{M}_{ow} \, \hat{M}_{wc})/(\hat{L}_w \, M_{oc}) \quad . \tag{12}$$

The real part of s in Eq. (10) represents the growth rate of the RWM. Equations (1) through (10) provide a general statement of the lumped parameter model. Much of the important physics is embedded in the mutual and self-inductance terms. These quantities must be determined in order to obtain quantitative or sometimes even qualitative results. An exact determination of these terms in 3-D geometry requires extensive numerical calculation.[22] However, a complete detailed formulation of the feedback stabilization problem which includes all the geometrical details goes beyond just the determination of these mutual and self-inductances. It is outside of the scope of the present work to discuss these issues.

Instead, we pursue further simplifications of the lumped circuit model. One simplification is provided by the cylindrical geometry, when the observation point is located on the wall as is the case of the RWM sensors in DIII-D.[16] The quantity Δ in Eq. (12) can be simplified by using the relation of mutual inductances, $M_{ij} = (r_i/r_j)^m$ for $r_i \leq r_j$. Here r_i and r_j can represent the radius of the plasma surface, the wall, the active coil or the observation sensor. These relationships give $\Delta = 0$ for the cylindrical limit. And Eq. (10) simplifies to

$$-\gamma_o^{-1} \, s + 1 = -G \, (\hat{M}_{oc}/M_{oc})/(1 - F \, G) \quad . \tag{13}$$

A further explicit evaluation of the mutual inductances in the cylindrical geometry yields

$$G = -(s\tau_w - \tau_w \, \gamma_o \,)(\, 1 - F \, G) \, . \tag{14}$$

In the present study, we also extend the model given by Jensen and Garofalo[18] to include the different feedback logic as well as assumptions on symmetry and boundary condition.[29] Arbitrary spacing of the wall, sensors, and active coils is in principle possible, but here we assume for simplicity that the sensors are located on the wall. Combining the equations describing the plasma response with that for the observation leads to

$$G = -(s \, \tau_w - \alpha \,)[1 - f_{comp} \, G/(1 + s \, \tau_w)] \quad (G > 0 \text{ stable}) \quad , \tag{15}$$

and

$$\alpha = \exp(-2kD)/[1 - \exp(-2kD)] \quad ,$$

where kD is a measure of the strength of the RWM mode , and $f_{comp}/(1 + s \, \tau_w)$ is analogous to F in the case of the full explicit mode logic [Eqs. (8–9)]. Thus, the Jensen/Garofalo model in the slab geometry is shown to be equivalent to the cylindrical limit of the Skin Current Model given in Eq. (14) when the observation sensor is located on the passive wall. For the experiment

analysis, these two models are used interchangeably. One advantage of the cylindrical and the slab geometry limit is that much of the results for the stability for the feedback of the RWM can be expressed readily in terms of the intuitively familiar parameters τ_w and γ_o, rather than the geometrical mutual inductances and the as yet to be determined mode strength L_{eff}.

For the controller gain, the standard proportional-integral-derivative (PID) format is used with,

$$G_{PID}(s) = [G_p + G_d\, s\, \tau_d/(s\, \tau_d +1) + G_i/(s\, \tau_i +1)]/(s\, \tau_p + 1) \quad , \tag{16}$$

where G_p, G_d and G_i are the proportional, differential and integral gains, respectively. The time constants, τ_p, τ_d, and τ_i are for proportional, differential and integral gains respectively. The power supply used for the experiment is current controlled with a compensation circuit to overcome the load impedance. After tuning the power supply to the active coils, the power supply gain transfer function G_{ps} is modeled by

$$G_{ps}(s) = G_{ps0}/[(st_{ps1} + 1)(st_{ps2} + 1)] \quad , \tag{17}$$

where τ_{ps1} and τ_{ps2} were determined from experimental measurements.

The overall total gain G is then

$$G(s) = G_{ps}(s)\, G_{PID}(s) \quad . \tag{18}$$

The unit used in Eq. (18) is set as Weber/Weber by adjusting the value of G_{ps0}. In another words, $G = 1$ stands for 1 Weber of flux produced at the sensors by the active coils due to 1 Weber of flux detected at the sensors.

We note that strictly speaking, the parameters employed in the present model should be computed from a detailed 3-D calculation. However, some of the equivalent mutual and self inductances used in this lumped parameter model can be estimated from vacuum field measurements. Others can be roughly estimated and adjusted from the actual spacing of the various elements. Despite the uncertainties associated with such estimates, these simple models allow us to qualitatively model the most of the important characteristics of RWM feedback control.

IV. THE FEEDBACK SYSTEM AND EXPERIMENTAL RESULTS FROM DIII-D

A.   Experimental set up

The present RWM feedback system on DIII-D consists of a pre-existing set of active control coils and a new of sensors designed for n = 1 RWM control as shown in Fig. 2. Six sensors (1.2 m height x 2.6 m width) are located on the midplane at the major radius side outside of but very close to the vacuum vessel. These loops detect the radial flux leakage through the vacuum vessel. Loops located 180 degrees apart are connected in anti-parallel to detect odd-n components. Six active coils are situated on the mid-plane and are toroidally in phase with the sensor loops. Coils 180 degrees apart are also paired in anti-parallel so that the feedback field produced by active coils contains only odd-n components. These active coil pairs are energized with three current controlled switching power amplifiers, each of which is capable of supplying up to 5 kA dc – 100 Hz. (Above 40 Hz the current is limited by the power supply voltage.) The active coil inductance is 225 μH with 10 mΩ resistance. A current of 1 kA produces 13 Gauss at the outboard midplane vessel wall. Up to 2 kA of the available current is typically used for quasi-dc
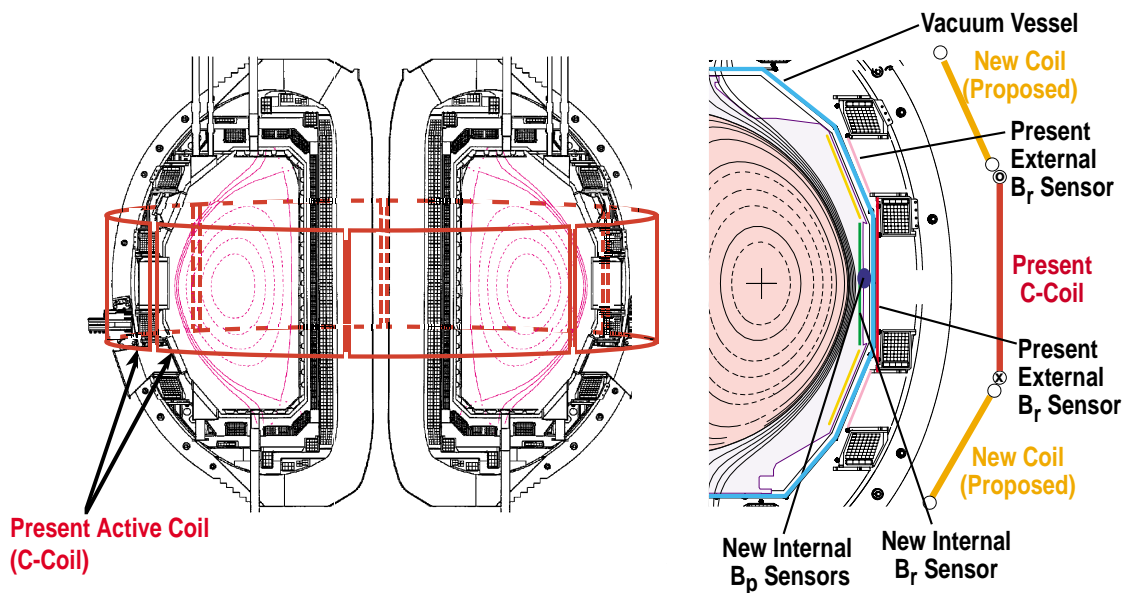
Fig. 2. The hardware arrangement, showing (a) present active coils and (b) present external B_r sensors. Also shown are new internal B_r and B_p sensors, now being installed, and a proposed extension of the active coil set.

error field correction. The parameters for the power supply response in Eq. (17) were $\tau_{ps1} \approx$ 0.1 ms and $\tau_{ps2} \approx 0.5$ ms. The controller is implemented digitally within the DIII-D digital plasma control system. The sampling rate is 50–100 μs and the digital calculation time for the standard PID algorithm is about 100 μs. Taking into account the PID calculation time, the proportional time constant, τ_p, in Eq. (16) is typically set to 0.4 ms in the experiment. VALEN and the VACUUM + GATO code results show that the longest eigenvalue of the eddy pattern is 7 ms without the plasma presence and the value decreases to 3.5 ms with the existence of plasma inside the vacuum vessel, although the value varies with plasma size. We chose 5 ms as an average reference value for the wall time resistive decay constant. Further description of hardware arrangement is given in Ref. 12.

B. Development of operation scenarios

The onset of ideal MHD depends on various parameters. In particular the onset condition near marginal stability is extremely sensitive not only to global parameters such as β_N and the internal inductance, ℓ_i, but also to the detailed local pressure- and current-profiles and their gradients. In the experiment, the profile characteristics at the RWM onset are produced through plasma transport evolving from the initiation of the discharge up to the time period of the MHD event. Thus, it is very difficult to prepare operational scenarios for the excitation or suppression of the ideal kink mode events in a routine manner. Nevertheless, an operation scenario is developed by utilizing the I_p-ramp to induce extra current density near the plasma edge[30,31] In this scenario, pre-heating NBI (P = 1.5 MW) was applied immediately after the discharge breakdown to increase plasma temperature and produce finite edge current density. This reduces the critical β_N for the ideal kink and facilitates easier plasma operation. The timing of the H–mode transition was adjusted to produce the pressure and q profiles which avoid other MHD events, such as neoclassical tearing modes. Finally, after a short period of 100–200 ms the I_p ramp has provided a large edge current density from which the RWM can be routinely produced. Sometimes, careful edge electron density control is necessary to maintain the edge current density for insuring a moderate value for the RWM growth rate. The I_p ramp was varied from 0.4 MA/s to 1.2 MA/s. The ratio of β_N to the no-wall β_N limit was typically 1.1 to 1.2 before the onset of the RWM.

C. The Smart Shell feedback logic

Figure 3 shows time traces of discharges with and without feedback. The feedback logic used is the Smart Shell logic with time derivative gain added. Without feedback, the RWM was excited at a low level (<1–1.5 Gauss) at 1350 ms. The amplitude slowly grew until t = 1385 ms with little
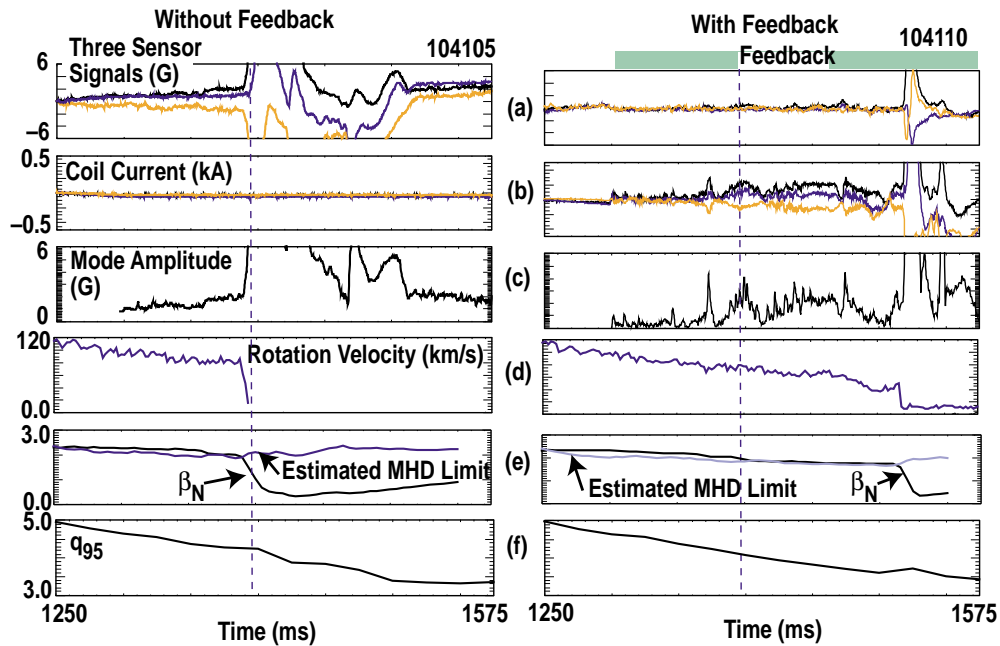
Fig. 3. The comparison of observations with/without feedback (104105/104110). (a) The three feedback sensor signals, (b) the active coil current, (c), mode amplitude, (d) the rotation velocity near q=2 surface, (e) normalized beta and estimated MHD limit, (f) the q-value at $\psi = 0.95$

reduction of plasma rotation velocity near the q = 2–3 surfaces. At t = 1385 ms, the RWM amplitude grew rapidly to over 10 Gauss with a growth time of 3–4 ms. At the onset of this fast RWM growth phase, a sudden loss of stored energy was observed. When the feedback was applied with G_p/G_d = 5/14, τ_p/τ_i = 0.4 ms/0.2 ms the flux leakage from the resistive wall, as measured by the total flux sensor, was observed to be kept near the noise level by the feedback flux compensation with an active coil current of 200–300 A (3–5 Gauss on the wall). After t = 1350 ms the mode started to show slow growth. At t =1390–1400 ms, when the major collapse occurred previously without feedback, some residual activity was observable on the feedback current trace as evidenced by the request for still higher current. Later the mode seemed to saturate at a level around 2 Gauss, although some bursts at 1430 ms were observed at the onset of the edge localized mode (ELM). Around t = 1500 ms, an oscillatory mode similar to a neoclassical tearing mode with 5–6 kHz (not shown) was observed. Mode locking of this oscillatory mode led to the major collapse at t = 1520 ms, presumably due to the combination of mode locking and the decrease in stability margin of the resulting configuration, as the discharge has been evolving with a rapid I_p ramp and a gradual decrease in the toroidal velocity.

Figure 4(a) shows the n=1 mode amplitude estimated from the flux loop signals and active coil currents vs. time for various differential gain settings and their relative durations as compared to the duration of the reference shot with no feedback. Without feedback, the configuration reached $\beta > \beta_{no.wall}$ at t = 1200–1210 ms. The duration of this higher β phase was 130 ms without feedback and it was prolonged to 270 ms with higher derivative gain. Without feedback the

M. Okabayashi, et al.
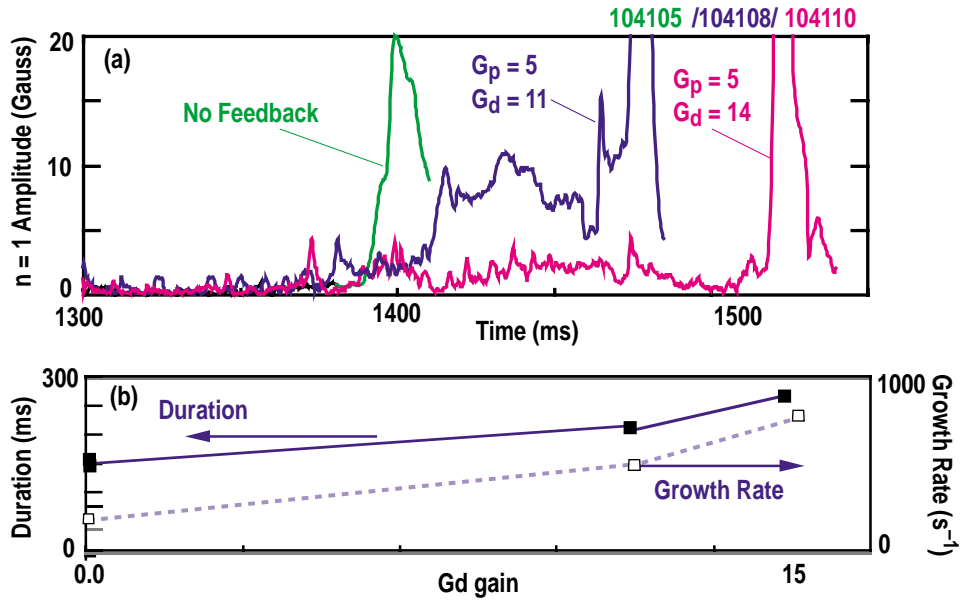
Fig. 4. (a) n=1 mode amplitude vs. time for various differential gains and (b) the dependence of RWM duration $\beta > \beta_{no.wall}$ and final RWM growth rate vs. the derivative gain.

mode amplitude grew to 20 Gauss with a growth time of 4-5 ms, whereas with feedback gain settings of $G_p/G_d = 5/11$ the mode amplitude tends towards a saturated value (≈ 10 Gauss). With further increase of the derivative gain setting to $G_p/G_d = 5/14$, the saturated amplitude was farther reduced to ≈ 1 Gauss, indicating that the RWM feedback system is working as expected. However, the final collapse time constant became faster with increased derivative gain. Figure 4(b) summarizes the variation of the duration of $\beta > \beta_{no.wall}$ and the mode growth rate at the final beta collapse as a function of the derivative gain. We observed that with the increase in the level of derivative gain, the growth rate was increased from 200–300 (s^{-1}) to 800–1000 (s^{-1}), edging closer to the ideal MHD growth time. This is presumably due to the shift of the equilibrium towards more ideal MHD unstable configuration due to the rapid I_p ramp. This observation is consistent with the hypothesis that the RWM is driven by the ideal MHD energy source.

D. Derivative and integral gains

Figure 5 shows the experimental results from implementing derivative and integral gains, and the prediction of these results from the lumped parameter model. (This figure also illustrates the reproducibility of the onset of the RWM with various gain settings. With the same gain settings, the onset of RWM was reproducible to within 20–30 ms.) With higher derivative gain, the discharge duration was prolonged and whereas with higher integral gain, the duration period was shortened. Figure 5(b) shows the predicted change in stability from Eq. (15). Since the RWM experiment in DIII-D requires parameters near the design limit of the power supply, operating
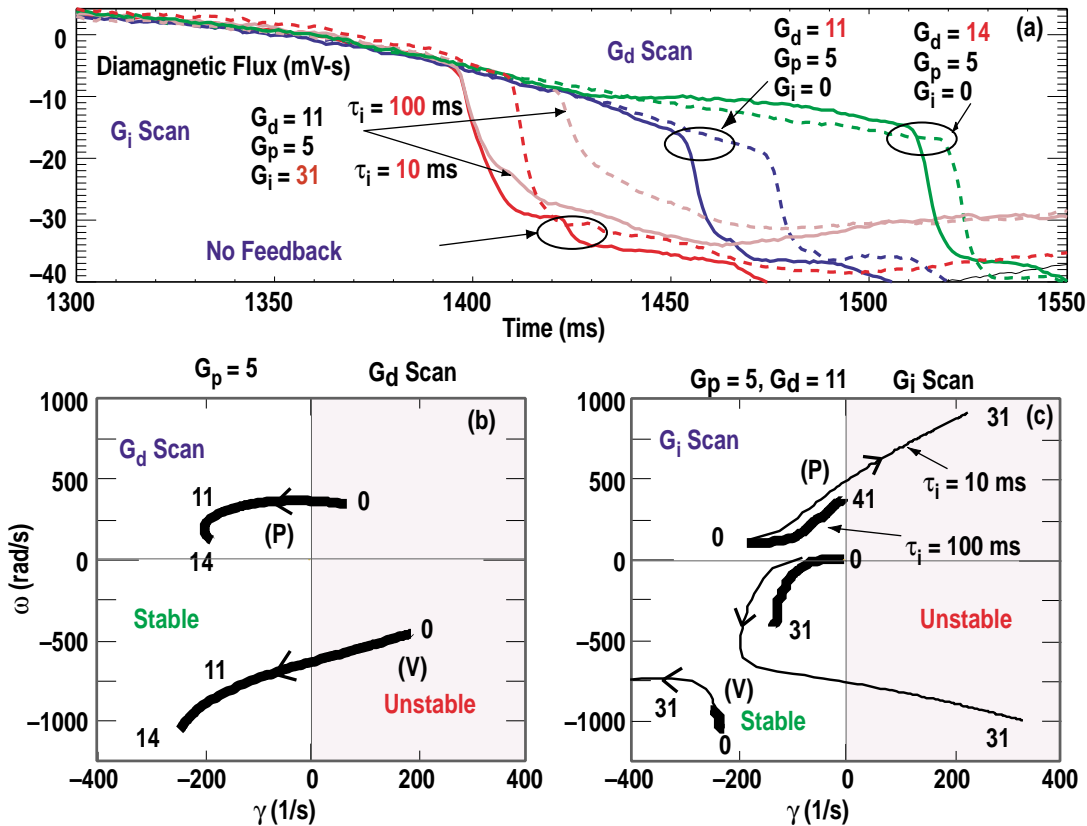
Fig. 5. (a) Diamagnetic flux (an indication of plasma beta) vs. time for derivative/integral gain scans with rapid I_p ramp. These are compared to predicted feedback behavior as shown in root-locus diagrams for (b) derivative scan and (c) integral scan. The time constant of $\tau_p/\tau_d = 0.4$ ms/0.2 ms for all discharges. The shots without feedback are 104105,104114, the shots with $G_p/G_d = 5/11$ are 104108/104109, the shots with $G_p/G_d = 5/14$ are 104110/104113, the shots with $G_p/G_d/G_i = 5/11/31$ are with $\tau_i = 100$ ms (104111) and with $\tau_i = 10$ ms (104112). The stability calculation was with kD = 0.092 and $\tau_w = 4$ ms.

characteristics of the power supply affect the plasma behavior: it was very important to include the power supply characteristics as realistically as possible. The power supply response was measured and numerically fitted to Eq. (17) in order to determine the power supply characteristic function G_{ps}. As shown in the derivative scan [Fig. 5(b)], without derivative gain, both the plasma mode branch (P) and the vacuum mode branch (V) started from the unstable domain. These modes were predicted to be stabilized according to the lumped parameter model at a derivative gain value close to the experimental settings. Further results from the simulation indicates that the experimental setting of $G_d = 11$–14 seems to have been optimally stabilizing for the plasma mode. In the experiment, in an attempt to improve the performance during the saturated period (1400–1500 ms), the value of the integral gain was also increased with fixed values of the proportional/differential gain ($G_p/G_d = 5/14$, $\tau_p/\tau_d = 0.4$ ms/0.2 ms, $\tau_i = 10$ ms and 100 ms). A negative experimental result was obtained. Results from the simulation indicates that the degradation of the stability with increased integral gain was too strong, as shown in Fig 5(c). Thus the lumped parameter model seems to be capable of explaining qualitatively the settings in

various feedback scenarios and can also be utilized to assist in parameter searches for improved performance.

E. Determination of the mode strength

So far in the stability analysis, it has been assumed that the mode strength is given a priori. From our experience in the stabilization of the vertical n=0 stability, it is important to estimate the experimental plasma mode strength, γ_o during the feedback process, since this parameter relative to the resistive wall time provides a practical gauge to the success of the feedback. A more successful feedback system operates with a large value of $\gamma_0 \tau_w$. The approach adopted here for finding γ_o is to solve the time dependent equations [Eqs. (1) through (3)] to match with the time behavior of the experimentally measured quantities, such as the observed flux or the feedback coil current. The mode strength γ_o serves as an adjustable unknown parameter in this matching process.

A simple way to achieve this matching is to note that the purpose of the feedback is to turn an exponentially growing RWM into an exponentially decaying mode. When the feedback is unsuccessful, due to the mode strength γ_o being too high, the RWM remains unstable. We also note that the feedback system is linear between its input and output and also that the actual experimental values of the input and output quantities satisfy the equations of the feedback circuit. In a numerical experiment, we can introduce a signal equal to the difference between the experimentally measured and the expected inputs to the feedback circuit, based on the assumed value γ_o. This procedure is summarized concisely below in notations with Laplace transformed variables for quantities in the cylindrical limit.

$$\Psi_{o.sim}(s) = (-\tau_w \gamma_o)^{-1} (-\gamma_o^{-1} s + 1)^{-1} M_{oc} [I_{c.sim}(s) - I_{c.exp}(s)] \quad , \tag{19}$$

$$I_{c.sim}(s) = -G_{ps}(s)G_{PID}(s) [\Psi_{o.sim}(s)/M_{oc}] \quad , \tag{20}$$

$$I_{c.sim}(s) = \Gamma(s)/[1 + \Gamma(s)] I_{c.exp}(s) \quad . \tag{21}$$

In Eqs. (19) through (21), the subscript sim has been used to denote quantities obtained in the time dependent solution. Eq (19) shows that only the difference between the $I_{c.sim}$ and $I_{c.exp}$ is used to produce $\Psi_{o.sim}(s)$; Eq. (20) is a recast of Eq. (14) for the simulated variables; and Eq. (21) shows the simulation coil current response to the experimentally measured current, $I_{c.exp}$ and $\Gamma(s) = G_{ps}(s)G_{PID}(s) (-\tau_w \gamma_o)^{-1} (-\gamma_o^{-1} s + 1)^{-1}$.

The time dependent solution of $I_{c.sim}(t)$ in Eq. (21) can be obtained numerically by the inverse Laplace transform with $s = \partial/\partial t$. An alternative formulation is based on $\Psi_{o.exp}$ or a com-

bination of $I_{c.exp}$ and $\Psi_{o.exp}$. The reason for choosing the experimental current $I_{c.exp}$ is that amongst all the physical quantities in the feedback system $I_{c.exp}$ contains the most dynamic frequency content whereas the measured flux $\Psi_{o.exp}$ is nearly zero and constant in time for the Smart Shell logic (Fig. 3). In this simulation, the value γ_o was adjusted to match the experimentally observed boundary
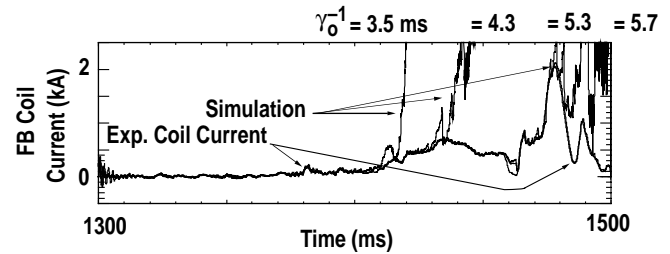
Fig. 6. Experimental feedback coil current, compared to numerical simulation predictions for several values of γ_o^{-1} (Shot 104108).

between stable and unstable operation. If the magnitude of γ_o chosen is too large, the time dependent calculation predicts an earlier onset of the unstable RWM. This is seen especially when the coil current $I_{c.exp}$ changes rapidly in time during its approach towards the experimentally observed onset of the RWM. With a γ_o chosen lower than the actual mode strength, the time dependent solution should be able to give results identical to the experimental observation. Therefore the maximum γ_o for which the solution remains stable through the experimental stable period should be adopted as a measurement of the strength of the mode in the actual experiment. The value, γ_o should be interpreted as a time-average over the duration of the simulation period and also be considered as a cylindrical geometry equivalent value, since Eq. (19) was formulated with the cylindrical assumption. Figure 6 shows results of simulations using four different settings for γ_o^{-1} applied to a shot (104108) with $G_p/G_d = 5/11$. Numerical calculations were done for all three feedback currents, including the actual mutual couplings between the three active coils and sensors. The highest value of γ_o or the lowest value of γ_o^{-1} (5.7 ms in this case), for which the simulation was stable throughout the experimental stable time, was found. The simulation barely remained stable up to the experimental onset time of 1470 ms if γ_o^{-1} is changed to 5.3 ms. This result indicates that a good approximation to the value of γ_o^{-1} in the experimental condition could be ≈ 5 ms.

F. Long duration feedback control

Figure 7 shows one of the long duration discharges (>50 times τ_w), produced by slow I_p-ramp operation with feedback, shot (104119). The growth of the RWM is expected to be more modest compared with the rapid I_p-ramp discharges. In this case, the full feedback gain was shut off for about 20 ms to observe the status of the RWM stabilization. Without feedback, shot (104118), the RWM mode grows slowly and at t = 1400 ms the amplitude reached 6–8 Gauss with a substantial reduction of the plasma rotation. With feedback, the amplitude was reduced to 1–2 Gauss. Signals from the feedback coil currents indicate that the RWM activity increased near t = 1470 ms and started to decrease slightly just before the feedback gain was turned off momentarily at t = 1500 ms. Here, the RWM mode behavior was determined from the soft x-ray
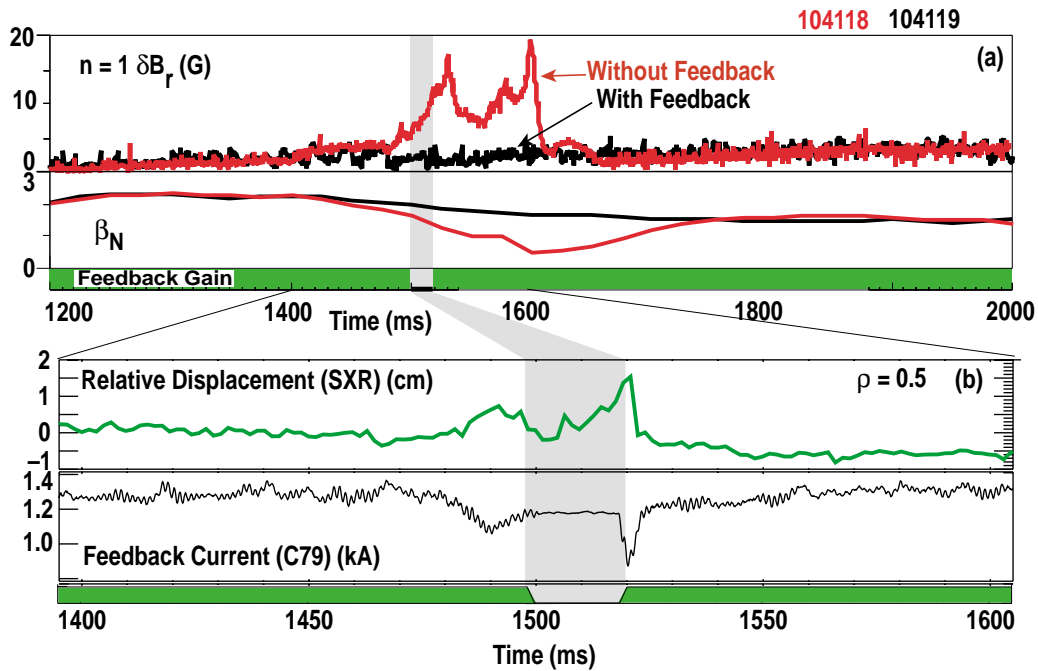
Fig. 7. (a) Comparison of RWM behavior with and without feedback during slow I_p ramp (104118, 104119), and (b) RWM onset during a brief interval with feedback gated off (104119).

array signals, S, located toroidally 150 degrees apart. The difference of these two profiles ΔS was normalized to provide the mode amplitude as the displacement length, $\xi = (dS/dr/\Delta S)^{-1}$. There was a slight mode excitation with the growth time of 30 ms before the feedback was turned off at $t = 1500$ ms. During the feedback-off period (1500–1520 ms), the RWM mode started to grow with a faster time constant of 10–13 ms and decayed quickly with the much shorter time constant of 1–2 ms when the feedback was resumed at $t = 1520$ ms. This sequence of controlled variation in feedback characteristics, during which the mode growth time constant before/during/after the gate-off also varies accordingly, indicates that the feedback has effectively controlled the RWM mode.

G. Explicit mode control

Explicit mode control is an approach optimized to increase the sensitivity to the plasma response. The terms M_{oc} and $(M_{ow} M_{wc}/M_{oc} L_w)$ in Eqs. (7) through (9) were obtained from measurements without plasma. Simple explicit mode control uses the feedback logic to compensate for the flux only due to the direct coupling to the feedback coil. However, over-compensation of the eddy current component near the frequency of τ_w^{-1} can make the feedback system oscillate. As shown in the stability analysis [Fig. 8(a)], with increase of the proportional gain, the stability condition shifts toward the stable regime with an oscillation frequency, $\omega/2\pi \approx$
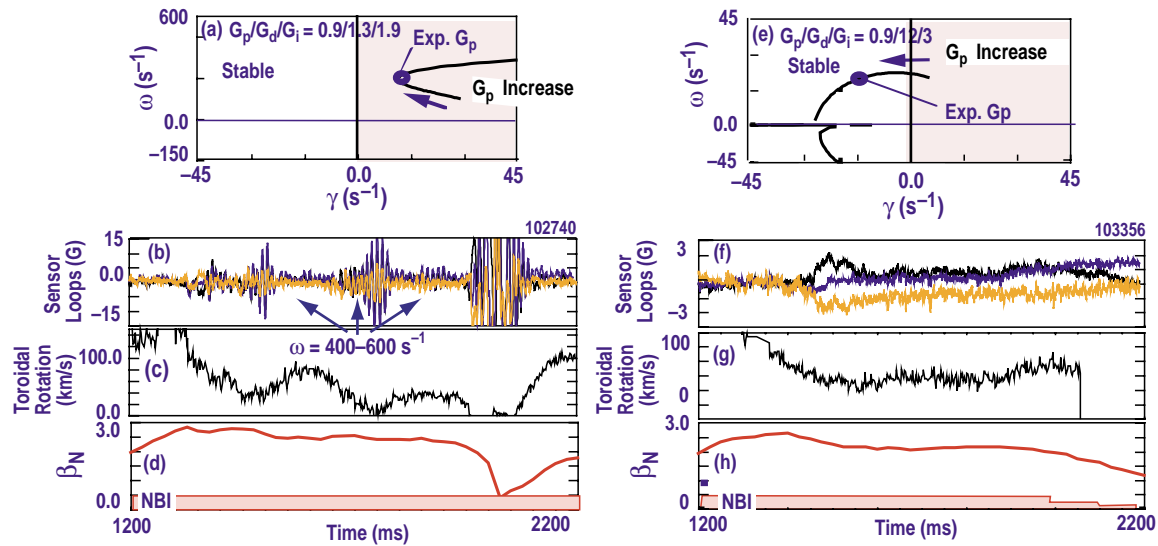
Fig. 8. (a) The stability analysis for the simple explicit mode control including only compensation due to the direct coupling to the active coil. The figures (b, c, d) are for the shot (102738) with the simple explicit mode control logic; (b) three sensor signals, (c) the rotation velocity at $\rho = 0.6$, (d) β_N, (e) The stability analysis for the full explicit mode control which include the eddy current compensation. The figures (f, g, h) are for the shot (103356) with full explicit mode control logic; (f) three sensor signals, (g) the rotation velocity at $\rho = 0.6$, (h) the β_N. The calculation was with $\gamma_o^{-1} = 10$ ms.

40–50 Hz. It is to be noted that whether the stability with higher gain is achievable depends on finer details in the system. With further increase of the gain, the operating condition, in general, shifts away from the stable domain. One of the best experimental results with this logic ($G_p/G_d/G_i = 0.9/1.5/1.2$ and $\tau_p/\tau_d/\tau_i = 0.4$ ms/0.4 ms/10 ms) is shown in Fig. 8(b-d). As the model predicts, a large amplitude oscillation was excited at RWM events. The observed frequency was 70–100 Hz ($\omega \tau_w = 2$–2.5), which is slightly higher than the values obtained from model predictions. In spite of these oscillations, the feedback system seems to have managed to stabilize the mode and the plasma rotation recovered each time after the RWM event occurred. This suggests that, although $\omega_{obs} \tau_w > 1$, the active coil currents did indeed interact through the wall. Compared with the simple explicit mode control, the full explicit mode control logic [Eqs. (8) and (9)] is expected to be stable with greatly reduced frequency [Fig. 8(e)]. The experimental results ($G_p/G_d/G_i = 0.8/12/3.1$ and $\tau_p/\tau_d/\tau_i = 1$ ms/0.4 ms/20 ms) [Fig. 8(f-h)] show that the condition of high beta continued for over the 700 ms without any oscillatory behavior.

These results indicate that the explicit mode control may have advantages, provided the compensation is done carefully. However, it remains as a task for the future to determine whether the full explicit mode control is more preferable for higher plasma performance. The experimental results also suggest that poloidal field sensors could serve as an alternative. Since poloidal sensors measure magnetic fields orthogonal to the radial field produced by the active coils, no compensation is required. Poloidal sensor loops located inside the vessel could also be more advantageous.

V. EXPERIMENTAL AND THEORETICAL ANALYSIS OF POSSIBLE MODE DISTORTION DURING THE FEEDBACK PROCESS

Mode rigidity is one of the most important issues that need to be addressed for a proper formulation of the feedback process. Here, we define mode rigidity as the invariance of the displacement of the mode during the feedback process.

The structure of the mode internal to the plasma was examined by utilizing two soft x-ray array systems 150 degrees apart in the toroidal direction. The structure of the mode in the vacuum was examined by flux loops located outside of the resistive vessel. Results of these measurements are shown in Fig. 9 for a representative discharge. According to observations from the flux loops located at the midplane, the amplitude of the RWM started to grow slowly at 1380 ms, reached 2–3 Gauss at 1410 ms, and saturated later at an amplitude of 10 Gauss. At 1475 ms, a major disruption took place. Figure 9 shows the soft x-ray array signals at the two different toroidal locations and the comparison between the derived displacement length ξ with the observed amplitude from the vacuum region [Section IV.F]. Note that the feedback was being applied from 1300 ms onward. The location of the displacement amplitude shown in Fig. 9(b) is at its maximum of $\rho = 0.5$. The close correlation in the behavior in time between the mode amplitudes outside of the vacuum vessel and that of the internal structure indicates that the

Fig. 9. The comparison of the n=1 mode displacement inside the vacuum vessel and the mode amplitude observed outside the vacuum vessel. (a) The soft x-ray array signals observed at two toroidal locations separated by 150 degrees in the toroidal direction. The locations are at $\rho = 0.86, 0.76, 0.63, 0.50, 0.37, 0.24$ and 0.11. (b) the displacement length at $\rho = 0.5$, (c) the mode amplitude measured outside the vacuum vessel.

RWM is a global mode with structure extending from the plasma core to the outside of the vessel. This characteristic agrees with the predictions from the ideal MHD theory. Furthermore,

the global mode pattern did not change significantly during the feedback process, as shown by the measurement of the external array of poloidal flux loops.

Figure 10 shows the time evolution of the mode structure derived from the midplane flux loops and another 24 off-midplane flux loops, and a comparison with and without feedback. The additional magnetic loops are similar to the feedback loop sensors except that these are off-midplane loops covering 30 degrees in toroidal angle and thus have better spatial resolution than the midplane loops which have 60 degrees toroidal coverage. In Fig. 10(b), the shots with and without feedback are normalized to give the same amplitude and toroidal phase on the midplane. The amplitude and phase from the other two off-midplane arrays have been found to be in very good agreement, showing that the feedback causes very little distortion to the mode structure even when the feedback is applied and the RWM has saturated.
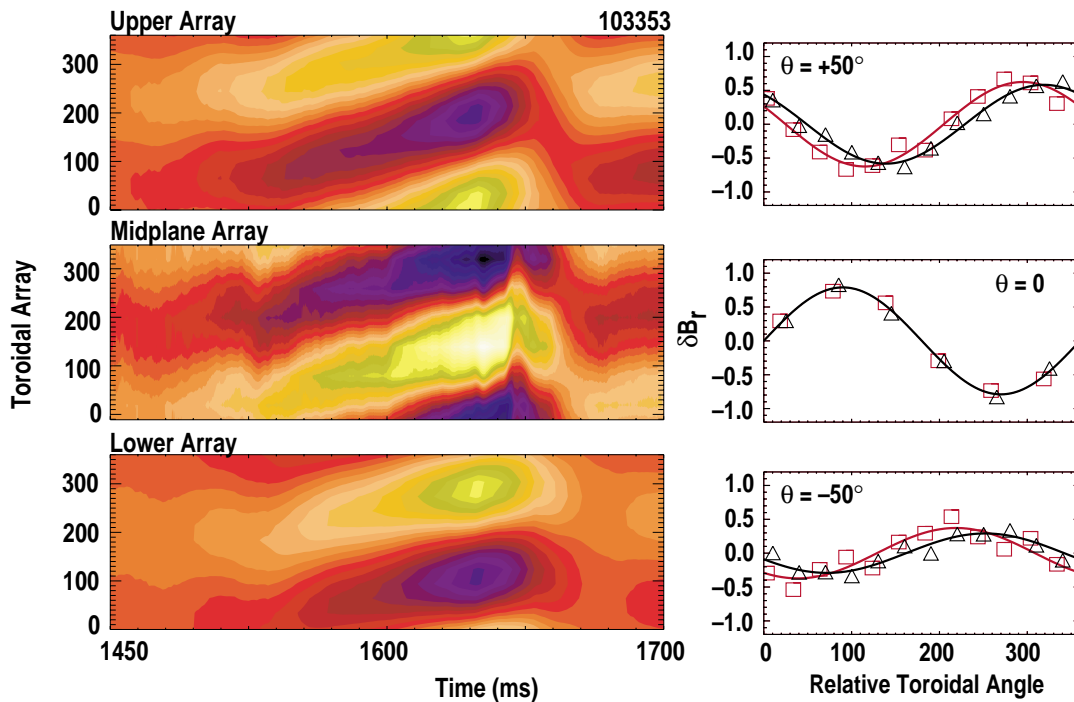
Fig. 10. (a) Time evolution of the external mode structure measured with three arrays of flux loops in a feedback-stabilized discharge (103355), and (b) comparison of external mode structure in the feedback-stabilized discharge (103355, squares) and a discharge without feedback (103353, triangles). δB_r is plotted vs. toroidal angle at the upper ($\theta = +50°$), midplane ($\theta = 0°$) and lower ($\theta = -50°$) arrays of flux loops. The two cases are normalized to give the same amplitude and phase at the midplane.

The rigidity of the plasma displacement during the feedback process has been studied theoretically by utilizing a new plasma stability package which couples the GATO ideal MHD stability code with the modified VACUUM code which includes the effect of feedback on a resistive wall. The detailed description of the formulations and applications of this code package

are discussed in Refs. [20] and [21]. Figure 11(a,b) shows the expected eddy current pattern without and with feedback. The eddy current pattern is not modified significantly with feedback except near the vicinity of the active coil. The accompanying plasma displacement throughout the plasma cross-section is not significantly modified either as shown in Fig. 11(c). It is seen that with feedback, the plasma displacement is only slightly more peaked towards the plasma center. Thus both theory and experiment support the assumption of mode rigidity, at least in the present experimental conditions.
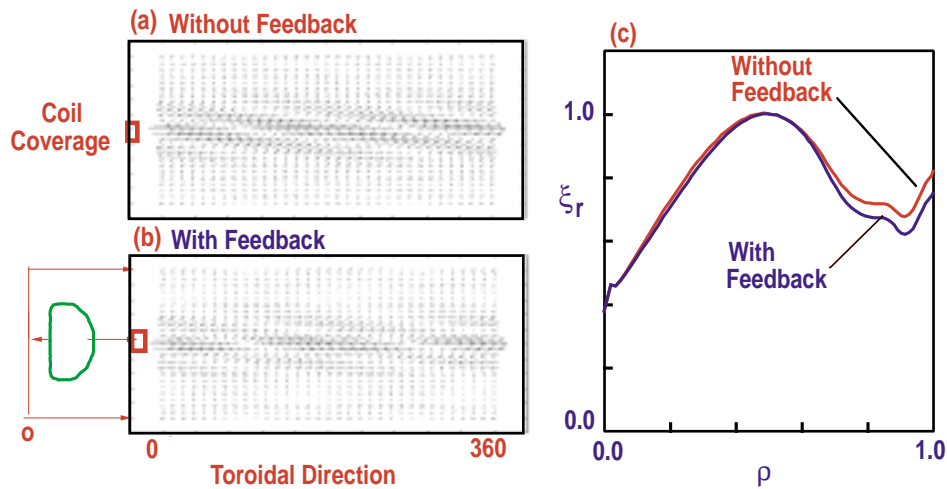
Fig. 11. Eddy current pattern on the resistive shell calculated with VACUUM + GATO code (a) without feedback and (b) with feedback. (c) the radial displacement length on the midplane.

VI. SUMMARY AND FUTURE PLAN

A summary of the experimental observations is as follows.

Utilizing reproducible RWM onset conditions and the rapid I_p ramp technique, it was demonstrated that Smart Shell logic can successfully suppress the RWM by reducing the flux leakage and maintaining the RWM amplitude small until the equilibrium evolves into an ideally less stable configuration (due to the rapid I_p ramp). With a weaker I_p-ramp, the β value in the discharge has been sustained above the no-wall limit for over 50–100 times the resistive flux loss time. The explicit mode control logic, which uses the signal only due to the plasma disturbance, has a potential advantage for feedback. Experimentally, the explicit mode logic performed at least as well as other control logic. The experimental observation from soft x-ray arrays and poloidal flux loops showed that the RWM structure is preserved throughout the present feedback process. The lumped model predictions are qualitatively consistent with the experiment measurements. It is significant to note that these agreements suggest that simplified models could be as useful for the feedback control of the RWM as has been the case with the control of $n = 0$ mode. Full MHD codes can be utilized to reduce uncertainties inherent in these simplified lumped parameter analysis.

Based on the present experimental results, a few suggestions for further improvements to facilitate future experiments can be made. One is the choice of locations for the feedback sensor loops and the other is the extent of poloidal coverage with the use of additional active coils. Direct measurement of the perturbed poloidal field through poloidal field B_p sensor loops would eliminate the extra compensation necessary in the explicit mode logic. Further advantages are expected if the loops are located inside of the vessel with increased sensitivity. Various combinations of these options have been studied with the VALEN code,[22] which can accommodate the actual three-dimensional geometry of the vacuum vessel, sensor loops, and active coils. The predicted achievements from various hardware upgrade options are summarized in Fig. 12. The cases shown are for a proposed feedback coil system with six upper and six lower coils placed adjacent to the present mid-plane coils. Sensor loop options utilized are poloidal and radial field sensors inside the vessel as shown in Fig.2. (Such sensors are now being installed.) The VALEN code predicts that the present feedback hardware arrangements can be about 20% effective as the ideal conducting wall in providing the increment in maximum stable β for the plasma. This corresponds to a no-feedback growth time $\gamma_o^{-1} \approx 10$ ms, which is consistent with the numerical simulation result (Section IV). When B_p (poloidal field) loops are used inside the vacuum vessel
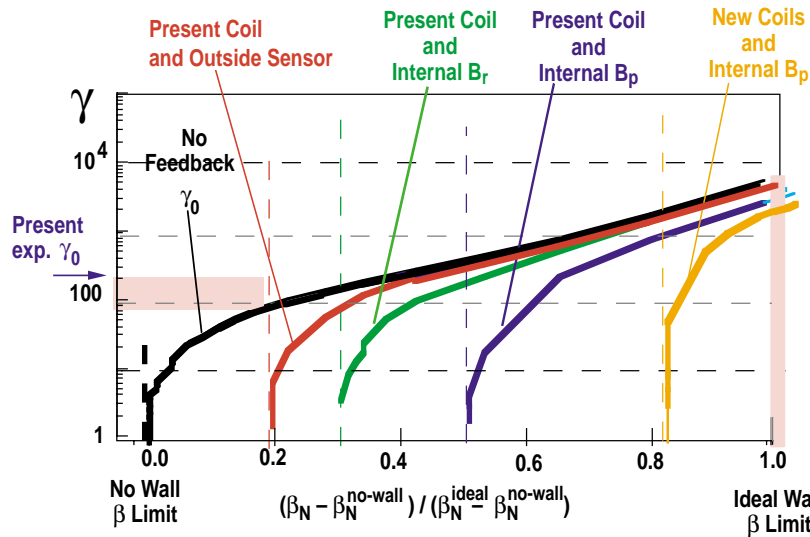
Fig. 12. Predicted growth rate vs. β with no feedback, present feedback configuration, and various options for next step with additional coils and new sensors.

with present coils, this effectiveness improves to about 50%. With internal B_p sensors and the proposed additional active coils, the effectiveness is further improved and can reach up to 80% of the stabilizing effect of a perfect conductor.

With the feedback system 80% as effective as the ideal wall, the growth rate of the RWM (with no feedback) is expected to have a time constant γ_o^{-1} near 0.5–1 ms $\approx$ (1/5 of τ_w). This is a challenging condition for the operation of the feedback system. This appears to be an extremely difficult extrapolation from the present achieved performance of γ_o^{-1} = 5–10 ms (1–2 τ_w). However, the present RWM control situation can be compared to the period when the n=0 control was initiated decades ago. Knowledge for n=0 control has been improved over decades; extremely elongated plasmas and high beta configurations (with $\gamma_o^{-1} \approx$ 0.1–0.2 τ_w) has become readily achievable in present day tokamaks. Control of the RWM should benefit from these accumulated experience for the control of n=0 mode. In summary, this proof of principle experiment has successfully identified the issues and established the fundamental direction for the next step experiments.

REFERENCES

[*]Current address: General Atomics, P.O. Box 85608, San Diego, California.
[a)]Princeton Plasma Physics Laboratory, Princeton, New Jersey.
[b)]Columbia University, New York, New York.
[c)]UKAEA-Culham Laboratory, Abingdon, United Kingdom.
[d)]Oak Ridge National Laboratory, Oak Ridge, Tennessee.
[e)]Lawrence Livermore National Laboratory, Livermore, California.

[1]B. Alper, M. K. Bevir, H. A. Bodin, et al., Plasma Phys. Control. Fusion **31**, 205 (1989).

[2]R. R. Goforth, T. N, Carlstrom, C. Chu, et al., Nucl. Fusion **26**, 515 (1986).

[3]E. J. Strait, Phys. Plasmas **1**, 1415 (1994).

[4]C. Kessel, J. Manickam, G. W. Rewoldt, and W. M. Tang, Phys. Rev. Lett. **72**, 1212 (1994); S. C. Jardin, C. E. Kessel, C. G. Bathke, et al., "Physics Basis for a Reversed Shear Tokamak Power Plant," Fusion Engineering and Design **38**, 27 (1997); A. D. Turnbull, et al., Phys. Rev. Lett. **74**, 718 (1995).

[5]J. P. Freidberg. *Ideal Magneto-Hydro-Dynamics*, (Plenum Press, New York ,1987) Chapter 9.

[6]T. S. Taylor, E. J. Strait, L. L. Lao, et al., Phys. Plasmas **2,** 2390 (1995).

[7]M. Okabayashi, N. Pomphrey, J. Manickam, et al., Nucl. Fusion **36**, 1167 (1996).

[8]T. Ivers, E. Eisner, A.M. Garofalo, et al., Phys. Plasmas **3**, 1926 (1996).

[9]E. J. Strait, T. S. Taylor, A. D. Turnbull, J. R. Ferron, L. L. Lao, B. W. Rice, O. Sauter, S. J. Thompson, and D. Wroblewski, Phys. Rev. Lett. **74**, 2583 (1995).

[10]A. M. Garofalo, A. D. Turnbull, E. J. Strait, M. E. Austin, J. Bialek, et al., Phys. Rev. Lett. **82**, 3811 (1999).

[11]E. J. Strait, A. M. Garofalo, M. E. Austin, et al., Nucl. Fusion **39**, 1977 (1999).

[12]A. M. Garofalo, E. J. Strait, J. M. Bialek, et al., Nucl. Fusion **40**, 1491 (2000).

[13]A. M. Garofalo, J. Bialek, A. H. Boozer, et al.*,* "Resistive Wall Mode Dynamics and Active Feedback Control in DIII-D," Proc. of 18th International Atomic Energy Agency Fusion Energy Conf., Sorrento, Italy, 2000, to be published in Nucl. Fusion.

[14]C. G. Gimblett and R. J . Hastie, Phys. Plasmas **7**, 258 (2000).

[15]A. H. Boozer, Phys. Plasmas **5**, 3350 (1998).

[16]M. Okabayashi, N. Pomphrey, and R. Hatcher, Nucl. Fusion **38**, 1607 (1998).

[17]T. H. Jensen, Phys. Plasmas **5**,192 (1998).

[18]T. H. Jensen and A. M. Garofalo, Phys. Plasmas **6,** 2757 (1999).

[19]E. A. Lazarus, J. B. Lister, and G. H. Neilson, Nucl. Fusion **30**, 111 (1990).

[20] M. S. Chance, M. Chu and M. Okabayashi, "Theoretical Modeling of the Feedback Stabilization of External MHD Mode in Toroidal Geometry," Proc. of 18th International Atomic Energy Agency Fusion Energy Conf., Sorrento, Italy, 2000, to be published in Nucl. Fusion.

[21] M. S. Chu, M. S, Chance and M. Okabayashi, Bull. Amer. Phys. Soc. **45**, 276 (2000)

[22] J. Bialek. Bull. Amer. Phys. Soc. **45**, 119 (2000).

[23] A. Bondeson and D. J. Ward, Phys. Rev. Lett. **72**, 2709 (1994).

[24] D. J. Ward and A. Bondeson, Phys. Plasmas **2**,1570 (1995).

[25] C. M. Bishop, Plasma Phys. Contr. Fusion **31**, 2641 (1989).

[26] R. Fitzpatrick and T. H. Jensen, Phys. Plasmas **3**, 2641 (1996).

[27] T. H. Jensen and R. Fitzpatrick, Phys. Plasmas **4**, 2997 (1997).

[28] Y. Q. Liu and A. Bondeson, Phys. Rev. Lett. **84**, 907 (2000).

[29] T. H. Jensen and A. M. Garofalo, private communication.

[30] A. M. Garofalo, E. Eisner, T. H. Ivers, et al., Nucl. Fusion **38**, 1029(1998).

[31] A. M. Garofalo, A. D. Turnbull, E. J. Strait, et al., Phys. Plasmas **6**, 1893 (1999).

ACKNOWLEDGMENT